2016 European Control Conference
June 29 - July 1, 2016. Aalborg, Denmark

Experiment Time Minimisation under Parameter Accuracy Constraints and Time-Domain Signal Amplitude Bounds

M.G. Potters, X. Bombois, Paul M.J. Van den Hof

Abstract— **We consider the input design problem of finding the minimal required experiment time such that accuracy constraints on the parameter estimate of an identification experiment are satisfied, while also respecting signal amplitude bounds. The input signal is parameterized as a multi-sine. We first show how multiple linear matrix inequalities from the least-costly and applications-oriented experiment design frameworks can be transformed into a generalised E-optimality constraint. Then, the solution to our problem is found by: (i) designing a multi-sine of one period with the Guillaume-Manchester algorithm [12], [10] that minimises the generalised E-optimality criterion under signal amplitude bounds, and (ii) utilising periodicity and an optimality condition to scale the experiment time such that the imposed accuracy constraints are also respected. An example shows an experiment time reduction of 50% compared with a traditional least-costly experiment design approach.**

I. INTRODUCTION

Classical works in optimal experiment design dealt with A-, D-, and E-optimality problems [7]. For example, the input was designed such that the determinant of the information matrix of the parameter estimate was maximised subject to an input power constraint. More recently, control-relevant problems were introduced in the *least-costly experiment design* [3] and *applications-oriented experiment design* [8] frameworks. In these problems, the experiment cost (usually a weighted sum of input and output powers) is minimised subject to one or more linear matrix inequality (LMI) constraints. The constraints impose quality conditions on the parameter estimate such that with a high probability good control performance can be guaranteed when using this estimate. Many problems in these two frameworks are convex and have consequently gained much interest.

In many real-life applications (e.g. industrial plants, medical analyses), however, amplitude bounds on the time-domain input and output signals are present. The convex methods [3], [8] formulated in the frequency domain, are therefore not suitable. Problems with time-domain amplitude signal constraints are difficult and non-convex, hence much less literature on this topic exists. Manchester [11] introduced an algorithm, applicable to open-loop systems, that maximises an A-, D-, or E-optimality criterion subject to input and output amplitude bounds. His main idea was to write the information matrix in quadratic forms in the input signal, and using a semidefinite relaxation. Building on [11], the authors of [6] proposed a novel method that combines an applications-oriented parameter estimate constraints and signal amplitude bounds. In [6], the objective was to minimise the experiment time while respecting amplitude bounds as well as a constraint on the covariance matrix of the to-be-identified parameter vector. The latter constraints ensures adequate accuracy for the design of a satisfactory controller. Their method converges to a (sub)optimal solution by cycling between two optimization problems, and is applicable to open-loop system identification. The same authors developed a graph-theory optimal experiment design method for closed-loop systems in [5], where it is assumed that the experiment is restricted to realisations of a stationary process with finite memory and alphabet.

In the present paper we consider the same optimal experiment design problem as in [6]. We however generalise their parameter accuracy constraint so that problems with other constraints arising in the least-costly experiment design framework [3] can be addressed. Our main contribution is nevertheless to propose an alternative method to solve this optimization problem. Our method is, contrary to [6], [11], applicable to open- and closed-loop identification.

To this end we consider a very general signal i.e. multi-sine signals, for which the amplitudes and phases of each harmonic need to be determined, and we make use of the fact that the problem in [6] is a generalised eigenvalue problem [4]. The parameter accuracy constraints are first transformed in an equivalent scalar one stating that the experiment time should be larger than the largest eigenvalue of a weighted covariance matrix of the parameter estimate. The amplitudes and phases of the multi-sine can then be determined by minimising the largest eigenvalue of this weighted covariance matrix while respecting the amplitude bounds on the input and output signals. This optimization problem can be efficiently solved with the nonlinear algorithm presented in [12], [10]. We provide analytical expressions for the gradients that support quick convergence of this algorithm, the derivation of which is more involved than in [10]. The minimal experiment time is then deduced straightforwardly as the optimal value of the objective function of this optimization problem, i.e.,

M.G. Potters is with Delft Center for Systems and Control, Delft University of Technology, 2628 CD Delft, The Netherlands m.g.potters@tudelft.nl

X. Bombois is with Laboratoire Ampère UMR CNRS 5005, Ecole Centrale de Lyon, 36 avenue Guy de Collongue, 69134 Ecully Cedex, France xavier.bombois@ec-lyon.fr

Paul M.J. Van den Hof is with the Department of Electrical Engineering, Eindhoven University of Technology, Postbus 513, 5600 MB, Eindhoven, The Netherlands p.m.j.vandenhof@tue.nl

The first and second author respectively thank B. Kuvshinov and G. Scorletti for fruitful discussions.

the largest eigenvalue of the weighted covariance matrix evaluated at the amplitudes of the optimal multi-sine.

II. PRELIMINARIES

Consider a discrete-time linear data-generating system, called the true system, defined by

$$u[n] = r[n] - C(q)y[n], \quad (1)$$
$$y[n] = G(q,\theta_0)u[n] + H(q,\theta_0)e[n], \quad (2)$$

where $r[n] \in \mathbb{R}$ is the to-be-designed excitation signal, $u[n] \in \mathbb{R}$ and $y[n] \in \mathbb{R}$ represent the discrete-time input and output of the true system, $e[n] \in \mathbb{R}$ a sampled white-noise with variance σ_e^2, $C(q)$ a linear, time-invariant controller, and $G(q,\theta_0)$ and $H(q,\theta_0)$ are stable, rational, finite-order transfer functions. Furthermore, $H(q,\theta_0)$ is monic and minimum phase. The sampling time $T_s = 1$ is chosen for notational brevity. The excitation signal is parameterised as a multi-sine with M harmonics:

$$r[n] = \sum_{m=1}^{M} A_m \sin(m\omega_f n + \phi_m), \quad (3)$$

in which A_m and ϕ_m are the amplitude and phase of the m^{th} harmonic, where $m = 1,\ldots,M$. We define $\mathbf{A} = \{A_m\}_{m=1}^M$, $\phi = \{\phi_m\}_{m=1}^M$ and $\Omega = \{\mathbf{A}, \phi\}$. The multi-sine is periodic with period $T = \frac{2\pi}{\omega_f}$ and has a fundamental frequency ω_f.

Suppose now that we apply N samples of the signal $\{r[n]\}_{n=1}^N$ to the true system. We collect the input and output data in the set $Z_N = \{u[n], y[n]\}_{n=1}^N$. The true parameter vector θ_0 can then be estimated using a full-order model structure $\mathscr{M} = \{G(q,\theta), H(q,\theta)\}$ with a prediction error method:

$$\hat{\theta}_N = \arg\min_{\theta} \frac{1}{N} \sum_{n=1}^{N} \varepsilon^2[n,\theta],$$

where $\varepsilon[n,\theta] = H^{-1}(q,\theta)\left(y[n] - G(q,\theta)u[n]\right)$ is the prediction error. In the limit $N \to \infty$ the estimate $\hat{\theta}_N$ will be asymptotically normally distributed around θ_0 under the conditions that (i) the true system $\{G_0(q) = G(q,\theta_0), H_0(q) = H(q,\theta_0)\} \in \mathscr{M}$, (ii) the excitation signal is sufficiently rich, and (iii) a delay is present in the controller or $G_0(q)$. Hence, in this limit $(\hat{\theta}_N - \theta_0) \to \mathscr{N}(0, \mathbf{P}_{N,\theta})$, where $\mathbf{P}_{N,\theta}$ is a positive-definite matrix defined by $\mathbf{P}_{N,\theta} = \frac{\sigma_e^2}{N}\bar{E}\left(\psi[n,\theta_0]\psi^T[n,\theta_0]\right)$, in which $\psi[n,\theta] \triangleq -\frac{\partial \varepsilon[n,\theta]}{\partial \theta}$, that can be estimated from $\hat{\theta}_N$ and Z_N. The expectation operator $\bar{E}$ is defined as $\bar{E}f[n] \triangleq \lim_{N\to\infty} \frac{1}{N}\sum_{n=1}^{N} Ef[n]$, where E is the traditional expectation operator. Using Parseval's relation a frequency-domain expression of $\mathbf{P}_{N,\theta}^{-1}$ for the input signal (3) can be deduced and reads [9]

$$\mathbf{P}_{N,\theta}^{-1}[\mathbf{A}] = \frac{N}{2\sigma_e^2} \sum_{m=1}^{M} A_m^2 \mathrm{Re}\left\{\mathbf{F}_r(e^{-im\omega_f},\theta_0) \times \mathbf{F}_r^*(e^{-im\omega_f},\theta_0)\right\} + \mathbf{R}_0, \quad (4)$$

where $\mathbf{P}_{N,\theta}$ is the covariance matrix for an experiment with N samples. For instance, if $N = 1$, then the corresponding covariance matrix is denoted by $\mathbf{P}_{1,\theta}$. Furthermore, the terms $\mathbf{F}_r$ and $\mathbf{R}_0$ in (4) are defined as

$$\mathbf{F}_r(e^{-im\omega_f},\theta_0) = H_0^{-1}(e^{-im\omega_f}) S_0(e^{-im\omega_f},\theta_0) \Lambda_G(e^{-im\omega_f})$$

and

$$\mathbf{R}_0 = \frac{N}{2\pi} \int_{-\pi}^{\pi} \mathbf{F}_v(e^{-i\omega},\theta_0)\mathbf{F}_v^*(e^{-i\omega},\theta_0)\, d\omega,$$

where $\mathbf{F}_v(e^{-i\omega},\theta_0) = H_0^{-1}(e^{-i\omega})\Lambda_H(e^{-i\omega}) - C(e^{-i\omega})S_0(e^{-i\omega})\Lambda_G(e^{-i\omega})$. In these equations, $S_0 = (1 + CG_0)^{-1}$ is the sensitivity function of the closed-loop system, $\Lambda_G(e^{-i\omega}) = \frac{\partial G(e^{-i\omega},\theta_0)}{\partial \theta} |_{\theta=\theta_0}$, $\Lambda_H(e^{-i\omega}) = \frac{\partial H(e^{-i\omega},\theta_0)}{\partial \theta} |_{\theta=\theta_0}$, and the asterisk denotes complex conjugation. The inverse of the covariance matrix is a strictly positive definite symmetric matrix, i.e. $\mathbf{P}_{N,\theta}^{-1} \succ \mathbf{0}$.

III. PARAMETER ACCURACY CONSTRAINTS

In the introduction we mentioned that we consider the optimal experiment design problem of [6]. The parameter accuracy constraint in [6] is of the form $\mathbf{P}_{N,\theta}^{-1} \succeq \mathbf{R}_{adm}$. Using the sensitivity analysis of [8] which is based on a second-order Taylor approximation, such a constraint guarantees an acceptable performence level for the loop made up by the true system and the controller designed with the identified model.

We can however be faced in practice with multiple constraints of the above type, i.e.,

$$\mathbf{P}_{N,\theta}^{-1}[\mathbf{A}] \succeq \mathbf{R}_{adm}(j) \text{ for all } j = 1,\ldots,J, \quad (5)$$

in which $J \in \mathbb{N}^+$ the number of constraints, the matrices $\{\mathbf{R}_{adm}(j)\}_{j=1}^J$ are symmetric and $(\kappa \times \kappa)$-dimensional, where $\kappa = \dim(\theta_0)$. The case in [6] corresponds to $J = 1$.

Multiple constraints (5) arise for instance when dealing with bounds on the individual variances of the parameter vector:

$$\forall j = 1,\ldots,J: \quad \mathbf{e}_j^T \mathbf{P}_{N,\theta}[\mathbf{A}]\mathbf{e}_j \le c_j, \quad (6)$$

where $J \le \kappa$, $\mathbf{e}_j$ the jth unit vector and $c_j \in \mathbb{R}^+$ the variance constraint for parameter θ_j. Using Schur's complement these constraints can be rewritten as

$$\forall j = 1,\ldots,J: \quad \mathbf{P}_{N,\theta}^{-1}[\mathbf{A}] \succeq \mathbf{R}_{adm}(j), \quad (7)$$

where $\mathbf{R}_{adm}(j) = \mathbf{e}_j \mathbf{e}_j^T c_j^{-1}$.

Multiple constraints also arise in the case where robustness analysis arguments are used to determine the largest additive uncertainty $r_{adm}(\omega)$ that can be allowed around the frequency response of the identified model to enable satisfactory robust control design. This leads to the following condition that has to hold at each frequency in $[0,\pi)$ (see e.g. [2]):

$$\forall \omega: \ |G(e^{-i\omega},\hat{\theta}_N) - G_0(e^{-i\omega})| < r_{adm}(\omega). \quad (8)$$

As shown in e.g. [1], the condition (8) at one particular frequency ω can be easily reformulated into a condition of the form $\mathbf{P}_{N,\theta}^{-1} \succeq \mathbf{R}_{adm}(\omega)$. This condition must in theory hold at each frequency, but a grid of the frequency range is often used instead, yielding a set of constraints as in (5), where J is the number of frequencies in the grid.

We recall that our goal is to minimize the experiment time N while respecting the constraints (5) and the amplitude constraints on the input u and output y of the closed-loop (1) during the identification experiment. In the introduction, we mentioned that we will solve this problem with the nonlinear optimization algorithm in [12], [10]. To apply this algorithm, we first need to transform the LMI constraints (5) into a single scalar one. This is done in the following lemma.

Lemma 1: Consider the LMI constraints in (5). These constraints are equivalent to the following scalar one:

$$N \geq \lambda_{max}\left(\mathscr{P}_{1,\theta}[\mathbf{A}]\mathscr{R}_{adm}\right). \tag{9}$$

with $\mathscr{P}_{1,\theta}$ and $\mathscr{R}_{adm}$ defined through the two $J\kappa \times J\kappa$-dimensional block-diagonal symmetric matrices

$$\mathscr{P}_{1,\theta}[\mathbf{A}] = \text{diag}(\mathbf{P}_{1,\theta}[\mathbf{A}],\ldots,\mathbf{P}_{1,\theta}[\mathbf{A}]) \succ \mathbf{0}, \tag{10}$$

$$\mathscr{R}_{adm} = \text{diag}(\mathbf{R}_{adm}(1),\ldots,\mathbf{R}_{adm}(J)), \tag{11}$$

in which $\mathbf{P}_{1,\theta}[\mathbf{A}]$ is the inverse of (4) for $N=1$.

Proof: Define $\mathbf{P}_{1,\theta}^{1/2} = (\mathbf{P}_{1,\theta}^{1/2})^T$ as the square root of $\mathbf{P}_{1,\theta}$. The constraint (5) for one particular j is equivalent to $\forall\theta : N\theta^T\mathbf{P}_{1,\theta}^{-1}\theta \geq \theta^T\mathbf{R}_{adm}(j)\theta$. Define the transformation $\theta_1 = S_1\theta$, where $S_1 = \mathbf{P}_{1,\theta}^{-1/2}$. Then this constraint may be written as $\forall\theta : N\theta_1^T\mathbf{I}\theta_1 \geq \theta_1^T\mathbf{P}_{1,\theta}^{1/2}\mathbf{R}_{adm}(j)\mathbf{P}_{1,\theta}^{1/2}\theta_1$, leading to

$$N \geq \lambda_{max}\left(\mathbf{P}_{1,\theta}^{1/2}\mathbf{R}_{adm}(j)\mathbf{P}_{1,\theta}^{1/2}\right). \tag{12}$$

The eigenvalues of the matrix in (12) are found by solving

$$\det\left(\mathbf{P}_{1,\theta}^{1/2}\mathbf{R}_{adm}(j)\mathbf{P}_{1,\theta}^{1/2} - \lambda\mathbf{I}\right) = 0. \tag{13}$$

Multiplying this equation from the left with $\det(\mathbf{P}_{1,\theta}^{1/2})$ and with $\det(\mathbf{P}_{1,\theta}^{-1/2})$ from the right and using $\mathbf{P}_{1,\theta}^{1/2}\mathbf{P}_{1,\theta}^{-1/2} = \mathbf{I}$ results in

$$\det(\mathbf{P}_{1,\theta}^{1/2})\det\left(\mathbf{P}_{1,\theta}^{1/2}\mathbf{R}_{adm}(j)\mathbf{P}_{1,\theta}^{1/2} - \lambda\mathbf{I}\right)\det(\mathbf{P}_{1,\theta}^{-1/2}) = 0 =$$

$$\det(\mathbf{P}_{1,\theta}\mathbf{R}_{adm}(j) - \lambda\mathbf{P}_{1,\theta}^{1/2}\mathbf{I}\mathbf{P}_{1,\theta}^{-1/2}) = \det(\mathbf{P}_{1,\theta}\mathbf{R}_{adm}(j) - \lambda\mathbf{I}),$$

which shows that $\forall i = 1,\ldots,\kappa : \lambda_i\left(\mathbf{P}_{1,\theta}^{1/2}\mathbf{R}_{adm}(j)\mathbf{P}_{1,\theta}^{1/2}\right) = \lambda_i\left(\mathbf{P}_{1,\theta}\mathbf{R}_{adm}(j)\right)$. The constraints (5) can be rewritten, using (12) and the previous equation, to

$$\forall j = 1,\ldots,J : N \geq \lambda_{max}\left(\mathbf{P}_{1,\theta}[\mathbf{A}]\mathbf{R}_{adm}(j)\right). \tag{14}$$

Equation (14) is equivalent to $N \geq \max\left[\lambda_{max}(\mathbf{P}_{1,\theta}\mathbf{R}_{adm}(1)),\ldots,\lambda_{max}(\mathbf{P}_{1,\theta}\mathbf{R}_{adm}[J])\right]$. Since $\mathscr{P}_{N,\theta}$ and $\mathscr{R}_{adm}$ are block-diagonal matrices we have

$$\det(\mathscr{P}_{1,\theta}\mathscr{R}_{adm} - \lambda\mathbf{I}_{J\kappa\times J\kappa}) = \prod_{j=1}^{J}\det(\mathbf{P}_{1,\theta}\mathbf{R}_{adm}(j) - \lambda\mathbf{I}_{\kappa\times\kappa}).$$

Thus, the $J\kappa$ eigenvalues of $\mathscr{P}_{1,\theta}[\mathbf{A}]\mathscr{R}_{adm}$ are equal to the eigenvalues of matrices $\mathbf{P}_{1,\theta}\mathbf{R}_{adm}(1),\ldots,\mathbf{P}_{1,\theta}\mathbf{R}_{adm}(J)$. The statement $N \geq \max\left(\lambda_{max}(\mathbf{P}_{1,\theta}\mathbf{R}_{adm}(1)),\ldots,\lambda_{max}(\mathbf{P}_{1,\theta}\mathbf{R}_{adm}(J)\right)$ is therefore equivalent to $N \geq \lambda_{max}(\mathscr{P}_{1,\theta}[\mathbf{A}]\mathscr{R}_{adm})$, see (9). This concludes the proof. ■

Remark 1: Although (12) could be used in the remainder of this text, it will be convenient to use (9) instead since this eigenvalue does not contain the square root of $\mathscr{P}_{1,\theta}$ in its argument. This property will be important in the Guillaume-Manchester algorithm that is used in Section IV.

IV. MINIMAL EXPERIMENT TIME ALGORITHM

Let us now formulate mathematically the optimization problem of [6] using Lemma 1 to replace the accuracy constraint with its scalar equivalent (9). The input and output signal amplitude bounds that we want to respect during the closed loop (1) identification are respectively u_{max} and y_{max}. This yields

$$\min_{\mathbf{A},\phi,N} N \tag{15}$$

subject to

$$f_u(\mathbf{A},\phi) \triangleq ||u_r(\mathbf{A},\phi)||_\infty/u_{r,max} \leq 1, \tag{16}$$

$$f_y(\mathbf{A},\phi) \triangleq ||y_r(\mathbf{A},\phi)||_\infty/y_{r,max} \leq 1, \tag{17}$$

$$N \geq \lambda_{max}\left(\mathscr{P}_{1,\theta}[\mathbf{A}]\mathscr{R}_{adm}\right), \tag{18}$$

where $||u_r(\mathbf{A},\phi)||_\infty = \max_n|u_r[n]|$ and $||y_r(\mathbf{A},\phi)||_\infty = \max_n|y_r[n]|$ represent the maximum absolute value of the noise-free input $u_r[n] = S_0(q)r[n]$ and output $y_r[n] = S_0(q)G_0(q)r[n]$ (i.e. the amplitudes), $\mathscr{R}_{adm}$ as defined in Section III, and $u_{r,max} \in \mathbb{R}^+$ and $y_{r,max} \in \mathbb{R}^+$ are the amplitude bounds of u_r and y_r:

$$u_{r,max} = u_{max} - \Delta u,\ \ y_{r,max} = y_{max} - \Delta y. \tag{19}$$

Here, Δu and Δy are user-chosen maximum noise disturbances caused on respectively $u[n]$ and $y[n]$. These deviations can be computed with for instance the simulation of $u_e[n] = -S_0(q)C(q)H_0(q)e[n]$ and $y_e[n] = S_0(q)G_0(q)H_0(q)e[n]$, where it is understood that $u[n] = u_r[n] + u_e[n]$ and $y[n] = y_r[n] + y_e[n]$.

Problem (15)-(18) is a Generalised EigenValue Problem (GEVP). The aim is to find the smallest value of N for which (16)-(18) are feasible for some values of N, $\mathbf{A}$, and ϕ. It is obvious that the optimal experiment time N^* and the optimal amplitudes $\mathbf{A}^*$ are related by the following optimality condition:

$$N^* = \lambda_{max}\left(\mathscr{P}_{1,\theta}[\mathbf{A}^*]\mathscr{R}_{adm}\right). \tag{20}$$

The solution to (15)-(18) is found with the following steps:

1) Solve the optimization problem

$$\min_{\{\mathbf{A},\phi\}} J = \lambda_{max}\left(\mathscr{P}_{1,\theta}[\mathbf{A}]\mathscr{R}_{adm}\right) \tag{21}$$

subject to

$$f_u(\mathbf{A},\phi) \leq 1,\ \ f_y(\mathbf{A},\phi) \leq 1, \tag{22}$$

where the objective function is the r.h.s. of the constraint (18), $f_u(\mathbf{A},\phi)$ and $f_y(\mathbf{A},\phi)$ defined in (16)-(17), $\mathscr{P}_{1,\theta}$ given by (10). This problem is solved with the Guillaume-Manchester algorithm detailed in Appendix A. Denote $\Omega^* = \{\mathbf{A}^*,\phi^*\}$ as the solution of this problem, and J^* as the minimum value of the objective function.

2) Use the optimality condition (20) to calculate the minimal experiment time:

$$N^* = J^* = \lambda_{max}\left(\mathscr{P}_{1,\theta}[\mathbf{A}^*]\mathscr{R}_{adm}\right). \tag{23}$$

This two-step approach is valid due to the special form of condition (20). It allows us to design $\mathbf{A}, \phi$ independently of N. It is obvious from inspecting (15)-(18) that the amplitudes $\mathbf{A}^*$ determined via (21)-(22) are the ones that fulfil the parameter accuracy constraint (18) with the smallest experiment time N. Moreover, since the excitation signal $r[n]$ is periodic, the signals $u_r[n]$ and $y_r[n]$ are also periodic with the same period. Consequently, it is sufficient to verify (22) over one single period of the excitation signal to guarantee that these constraints hold for any experiment length N. This is how (21)-(22) is solved in Appendix A.

The optimal excitation signal $\{r_{opt}[n]\}_{n=1}^{N}$ (c.f. (3)) used for identification is then defined by $N = N^*$ and $\Omega = \Omega^*$ that are found with steps 1) and 2).

Remark 2: In some problems the matrix $\mathscr{R}_{adm}$ is non-singular. In that case, the constraints $\forall j = 1,\ldots,J$: $\boldsymbol{P}_{N,\theta}^{-1}[\boldsymbol{A}] \succeq \boldsymbol{R}_{adm}(j)$ in Section III can be recast into the single constraint $\lambda_{min}(\mathscr{P}_{N,\theta}^{-1}[\boldsymbol{A}]\mathscr{R}_{adm}^{-1}) \geq 1$, see [13] for the derivation. Consequently, the constraint (18) may be replaced with $N\lambda_{min}(\mathscr{P}_{1,\theta}^{-1}\mathscr{R}_{adm}^{-1}) \geq 1$, and the optimality condition (20) becomes $N^*\lambda_{min}(\mathscr{P}_{1,\theta}^{-1}[\boldsymbol{A}^*]\mathscr{R}_{adm}^{-1}) = 1$. Furthermore, the objective function in (21) becomes $-\lambda_{min}(\mathscr{P}_{1,\theta}^{-1}[\boldsymbol{A}]\mathscr{R}_{adm})$ and (23) is changed to

$$N^* = \frac{1}{\lambda_{min}(\mathscr{P}_{1,\theta}^{-1}[\boldsymbol{A}^*]\mathscr{R}_{adm}^{-1})}. \tag{24}$$

It can be beneficial to use this different criterion if $\mathscr{R}_{adm}$ is non-singular as the convergence of the Guillaume-Manchester algorithm may be quicker due to a simpler eigenvalue gradient.

V. NUMERICAL EXAMPLE

In this section we consider a four-parameter open-loop (i.e. $C(z) = 0$ and $S(z) = 1$) system

$$G(z,\theta_0) = \frac{\theta_1 z^{-1} + \theta_2 z^{-2}}{1 + \theta_3 z^{-1} + \theta_4 z^{-2}}, \tag{25}$$

that connects the input $u[n]$ to the output $y[n]$, and where $\theta_0 = \{0.8, 0, -0.9854, 0.8187\}$. Furthermore, we use the noise model $H(z) = 1$ (thus $\mathbf{R}_0 = 0$ in (4)), noise variance $\sigma_e^2 = 1.12$, and a sampling time $T_s = 0.8$s. We consider an accuracy constraint defined by $J = 1$ and $\mathbf{R}_{adm} = 10^4\mathbf{I}_{4\times4}$, i.e. $\mathbf{P}_{N,\theta}^{-1} \succeq \mathbf{R}_{adm} = 10^4\mathbf{I}_{4\times4}$. The input and output signal constraints are $u_{r,max} = 1$ and $y_{r,max} = 10^3$ (effectively, only the input constraint is active), and we take for convenience $\Delta u = \Delta y = 0$.

In this example, we show the advantage of using the approach presented in the previous section with respect to a design that would consist of using a classical design with power constraints and scaling subsequently the results to respect amplitude constraints. To this end, we compare the minimum time of (15)-(18) with the problem (26)-(29), in which $\mathscr{R}_{adm} = \mathbf{R}_{adm}$ defined previously, $\gamma_u = 1, \gamma_y = 1000$, and of which the optimal amplitudes are scaled to $\mathbf{A}_{LCED}^*$ using (31) to satisfy the input and output amplitude constraints. The optimal experiment length found with (26)-(29) is then subsequently scaled to N_{LCED}^*, which ensures that (18) is also satisfied. The optimal phases ϕ_{LCED}^* are selected using Schroeder phases, see (30). The LCED-like solution $A_{LCED}^*, \phi_{LCED}^*$ is also used to initialise the Guillaume-Manchester algorithm for $p = 2$, see Appendix A, for which we furthermore define $L = 1000$, and $p_{end} = 64$. The multi-sine $r[n]$ used in both methods is defined by its fundamental frequency $\omega_f = 0.07$ rad/s and $M = \pi/(\omega_f T_s) = 56$ harmonics.

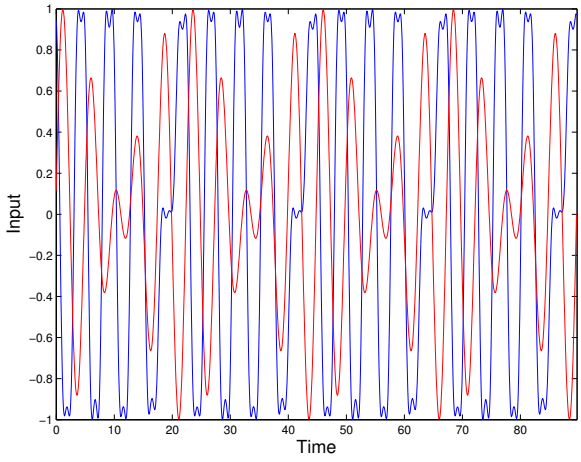

Fig. 1. Time domain realisation of optimal excitation signal r using the minimal time algorithm (blue) and classical LCED method (red). One full period of both signals is displayed.

The optimal input spectrum of the minimum time and LCED solutions are respectively shown in blue and red in Fig. 2 and their time-domain realisations in Fig. 1. We see that the two frequencies corresponding to the smallest sum of amplitudes in the LCED formulation are also present in the minimum time solution, albeit excited with a much higher amplitude. This is possible due to the freedom in phase selection that reduces the amplitude of the input signal. Furthermore, this freedom also allows for additional higher frequencies rendering the signal more square-shaped. To satisfy the input and output bounds, as well as the accuracy constraint, the LCED solution requires $N = 10^4$ samples, whereas for the minimum time solution only needs $N = 5045$, a reduction of almost 50%.

VI. CONCLUSIONS

We considered the problem of finding the minimal experiment time satisfying parameter accuracy constraints and input and output amplitude bounds. We first showed how to cast several LMI constraints into a single scalar one. Using this result we derived an optimality condition that, in conjunction with a non-convex algorithm based on [12], [10], solved the above problem. In contrast to previous works, our method can be applied to open- and closed-loop discrete- and continuous-time systems. Although the algorithm is

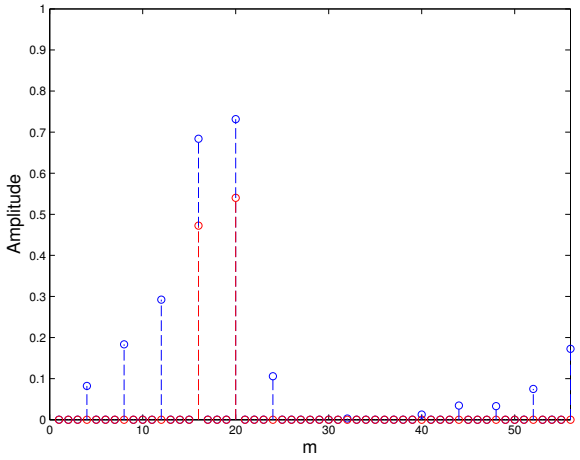

Fig. 2. The optimal input spectrum resulting from the minimal time algorithm (blue) and the optimal spectrum found with the classical LCED method (red).

non-convex, good results are obtained. An example showed an experiment time reduction of 50% compared with a classical least-costly experiment design approach. We have also applied the algorithm to complex physical models, and found experiment time reductions exceeding 40% [13].

An interesting future direction is to compare our method to the existing ones [11], [6], [5], and analyse how the experiment time reduction scales with the number of unknown parameters.

REFERENCES

[1] X. Bombois and G. Scorletti. Design of least-costly identification experiments - the main philosophy accompanied by illustrative examples. *Journal Europeen des Systems Automatises*, 46(6):587–610, 2012.

[2] X. Bombois, G. Scorletti, M. Gevers, R. Hildebrand, and Paul M.J. Van den Hof. Cheapest open-loop identification for control. In *Proceedings of the 43th IEEE Conference on Decision and Control*, December 2004.

[3] X. Bombois, G. Scorletti, M. Gevers, P.M.J. Van den Hof, and R. Hildebrand. Least costly identification experiment for control. *Automatica*, 42:1651–1662, 2006.

[4] S. Boyd, L. El Ghaoui, E. Feron, and V. Balakrishnan. *Linear Matrix Inequalities in System and Control Theory*. SIAM.

[5] A. Ebadat, P.E. Valenzuela, C.R. Rojas, H. Hjalmarsson, and B. Wahlberg. Applications-oriented input design for closed-loop system identification: A graph-theory approach. In *Proceedings of the 2014 IEEE Conference on Decision and Control*, Los Angeles, December 2014.

[6] A. Ebadat, B. Wahlberg, H. Hjalmarsson, C. Rojas, P. Hägg, and C.A. Larsson. Applications oriented input design in time-domain through cyclic methods. In *19th IFAC World Congress*, Capte Town, South Africa, August 2014.

[7] G.C. Goodwin and R.L. Payne. *Dynamic System Identification: Experiment Design and Data Analysis*. Academic Press, 1977.

[8] H. Hjalmarsson. System identification of complex and structured systems. In *Proceedings of the European Control Conference 2009*, pages 3424–3452, Budapest, Hungary, 2009.

[9] L. Ljung. *Systems Identification: Theory for the User*. Prentice Hall, 1999.

[10] I.R. Manchester. An algorithm for amplitude-constrained input design for system identification. In *Proceedings of the 48th IEEE Conference on Decision and Control*, 2009.

[11] I.R. Manchester. Input design for system identification via convex relaxation. In *Proceedings of the 49th IEEE Conference on Decision and Control*, pages 2041–2046, December 2010.

[12] Guillaume P., J. Schoukens, R. Pintelon, and I. Kollar. Crest-factor minimization using nonlinear chebyshev approximation methods. *IEEE Transactions on Instrumentation and Measurement*, 40(6):982–989, December 1991.

[13] M.G. Potters. *Experiment Design for Identification of Linear Structured Systems, PhD thesis, to be printed*. 2016.

[14] N.P. van der Aa, H.G. ter Morsche, and R.R.M. Mattheij. Computation of eigenvalue and eigenvector derivatives for general complex-valued eigensystem. *The Electronic Journal of Linear Algebra*, 16:300–314, 2007.

APPENDIX

A. Guillaume-Manchester Algorithm

In this appendix we solve (21)-(22) using the Guillaume-Manchester algorithm defined below. We refer the reader to [12], [10] for more details. Conceptually, the idea is to solve (21)-(22) iteratively by replacing the amplitude of u_r, y_r by the p-norms of these signals and by increasing the value of p at each iteration. We have indeed that the maximal amplitude of a a signal is given by its p-norm for $p = \infty$.

Before presenting the algorithm, we make two observations. First, since r is a multi-sine, the signals u_r and y_r are also multi-sines (with the same period). Consequently, we have to only consider one period of these signals to verify the amplitude constraints. Second, if the actual sampling frequency is not very high, taking the maximal values of $u_r[n]$ and $y_r[n]$ may result in poor estimates of the actual amplitudes of their continuous-time equivalents. However, we are not obliged to use the actual sampling frequency to solve (21)-(22). We can artificially increase the sampling frequency to more accurately determine the amplitudes by deducing analytically the continuous-time expressions of u_r and y_r. We assume that the excitation signal r is also continuous and that the discrete-time closed-loop transfer functions relating r with u_r, y_r are equal to their continuous-time counterparts in the frequency range $[0, \pi]$ (we assume $T_s = 1$ for simplicity). With these analytical expressions we can sample these signals at any sampling rate. Let us assume that for this high sampling frequency, $L+1$ is the number of samples of one period of r, u_r and y_r. In the sequel, we will subsequently compute the p-norms of u_r, y_r for the Guillaume-Manchester algorithm using $u_r[l]$ and $y_r[l]$ for $l = 0, \ldots, L$.

The Guillaume-Manchester algorithm is defined as follows. The input and output signals are constructed with the amplitudes and phases, i.e. Ω, of the excitation signal r. We define $\mathbf{A}_p = \{A_1, \ldots, A_M\}_p$ and $\phi_p = \{\phi_1, \ldots, \phi_M\}_p$ as its amplitude and phase variables at step $p \in [2, 4, 8, \ldots, p_{end}]$, and their elements are denoted by $A_{p,m}$ and $\phi_{p,m}$.

Initialisation. Select the fundamental frequency ω_f and number of harmonics M of the multi-sine $\{r[l]\}_{l=0}^{L}$ (3). The solution for $p = 2$ is $\{\mathbf{A}_2^*, \phi_2^*\} = \Omega_2^*$ and given by the user. It initialises the Guillaume-Manchester algorithm. One way to initialise Ω_2^* is to solve a LCED-like problem [3]. Define the multi-sine (3) for the user-chosen values ω_f and M and solve the Generalised EigenValue Problem (GEVP):

$$\min_{\mathbf{A}} N \tag{26}$$

subject to

$$\frac{1}{2}\sum_{m=1}^{M}|S_0(e^{-im\omega_f})|^2A_m^2 \le \gamma_u, \tag{27}$$

$$\frac{1}{2}\sum_{m=1}^{M}|S_0(e^{-im\omega_f})|^2|G_0(e^{-im\omega_f})|^2A_m^2 \le \gamma_y, \tag{28}$$

$$N\mathscr{P}_{1,\theta}^{-1}[\mathbf{A}] \succeq \mathscr{R}_{adm}, \tag{29}$$

where γ_u, γ_y are bounds on respectively the input and output power, and the last constraint equal to (18). In solving the above optimization problem frequencies for which the system is sensitive to changes its parameters are selected, leading to the smallest N.

Furthermore, we define the phases at $p = 2$ using Schroeder phases (see also [10]), i.e.,

$$\phi_{2,m}^* = -2\pi\sum_{q=1}^{m-1}(m-q)A_{2,m}^*, \tag{30}$$

which reduce the amplitudes of the input and output signals.

The optimal amplitudes from the above problem and the phases $\phi_{2,m}^*$ are then used to design $\{u_r[l]\}_{l=0}^L$ and $\{y_r[l]\}_{l=0}^L$. To ensure that the constraints (16)-(17) are respected, the amplitudes are then uniformly scaled until we have the solution Ω^* for which either $f_u(\Omega_2^*) = 1$ or $f_y(\Omega_2^*) = 1$ (see (31)), and N is subsequently scaled such that (18) is furhermore respected.

We note that random phase and amplitude selection is another possibility to initialise Ω_2^*.

Iterative steps. Solve for $p = 4, 8, 16, \ldots, p_{end}$ the following optimization problem:

Use the solution of previous step, $\mathbf{A}_{p/2}^*$ and $\phi_{p/2}^*$, and scale to fit constraints and provide the next initial guess:

$$\mathbf{A}_p = \frac{\mathbf{A}_{p/2}^*}{\max\left[f_{u,p}(\mathbf{A}_{p/2}^*, \phi_{p/2}^*), f_{y,p}(\mathbf{A}_{p/2}^*, \phi_{p/2}^*)\right]}, \tag{31}$$

$$\phi_p = \phi_{p/2}^*, \tag{32}$$

where $f_{u,p} = ||u_r(\mathbf{A}, \phi)||_p^p$, $f_{y,p} = ||y_r(\mathbf{A}, \phi)||_p^p$, and $||x(k)||_p \triangleq \left(\frac{1}{K}\sum_{k=1}^K |x(k)|^p\right)^{1/p}$. Then solve

$$\mathbf{A}_p^*, \phi_p^* = \arg\min_{\{\mathbf{A}_p, \phi_p\}} \lambda_{max}\left(\mathscr{P}_{1,\theta}[\mathbf{A}_p]\mathscr{R}_{adm}\right) \tag{33}$$

subject to

$$f_{u,p}(\mathbf{A}_p, \phi_p) \le 1, \quad f_{y,p}(\mathbf{A}_p, \phi_p) \le 1. \tag{34}$$

The solution to (21)-(22) in Section IV is provided by the solution of the Guillaume-Manchester algorithm and is denoted by $\Omega^* = (\mathbf{A}_{p_{end}}^*, \phi_{p_{end}}^*)$.

B. Gradients for the Guillaume-Manchester Algorithm

The gradients of the objective function and constraints can be numerically computed with the *fmincon* function used to solve (21)-(22). However, the speed of convergence can be greatly improved when providing *fmincon* with analytical gradients. Here these gradients are provided.

Objective function in (33): We assume that the eigenvalues of matrix $\mathscr{P}_{1,\theta}\mathscr{R}_{adm}$ are simple, and that this matrix is non-defective. For non-simple eigenvalues, we refer the reader to the methods detailed in [14]. Denote $\mathbf{v}_{max}$ as the right eigenvector corresponding $\mathscr{P}_{1,\theta}\mathscr{R}_{adm}$, i.e., we have

$$\left(\mathscr{P}_{1,\theta}[\mathbf{A}_p]\mathscr{R}_{adm}\right)\mathbf{v}_{max}[\mathbf{A}_p] = \lambda_{max}[\mathbf{A}_p]\mathbf{v}_{max}[\mathbf{A}_p]. \tag{35}$$

Furthermore, define $\mathbf{w}_{max}$ as the right eigenvector of $(\mathscr{P}_{1,\theta}\mathscr{R}_{adm})^T$, i.e., $\mathbf{w}_{max}^T$ is the left eigenvector of $\mathscr{P}_{1,\theta}\mathscr{R}_{adm}$:

$$\mathbf{w}_{max}^T[\mathbf{A}_p]\left(\mathscr{P}_{1,\theta}[\mathbf{A}_p]\mathscr{R}_{adm}\right) = \lambda_{max}[\mathbf{A}_p]\mathbf{w}_{max}^T[\mathbf{A}_p]. \tag{36}$$

We normalise the vectors $\mathbf{w}_{max}$ and $\mathbf{v}_{max}$ such that $\mathbf{w}_{max}^T\mathbf{v}_{max} = 1$. Denote $\mathbf{B}[\mathbf{A}_p] = \mathscr{P}_{1,\theta}[\mathbf{A}_p]\mathscr{R}_{adm}$, then taking the derivative of (35) w.r.t. $A_{p,m}$ on both sides results in

$$\left(\frac{\partial}{\partial A_{p,m}}\mathbf{B}[\mathbf{A}_p]\right)\mathbf{v}_{max}[\mathbf{A}_p] + \mathbf{B}[\mathbf{A}_p]\left(\frac{\partial}{\partial A_{p,m}}\mathbf{v}_{max}[\mathbf{A}_p]\right) = \left(\frac{\partial}{\partial A_{p,m}}\lambda_{max}[\mathbf{A}_p]\right)\mathbf{v}_{max}[\mathbf{A}_p] + \lambda_{max}[\mathbf{A}_p]\left(\frac{\partial}{\partial A_{p,m}}\mathbf{v}_{max}[\mathbf{A}_p]\right).$$

Multiplying both sides with $\mathbf{w}_{max}^T$ from the left and using (36), $\mathbf{w}_{max}^T\mathbf{v}_{max} = 1$, and the definition of $\mathbf{B}[\mathbf{A}_p]$, we obtain

$$\frac{\partial}{\partial A_{p,m}}\lambda_{max}[\mathbf{A}_p] = -\mathbf{w}_{max}^T[\mathbf{A}_p]\Bigg(\mathscr{P}_{1,\theta}[\mathbf{A}_p]\times \frac{\partial}{\partial A_{p,m}}\left(\mathscr{P}_{1,\theta}^{-1}[\mathbf{A}_p]\right)\mathscr{P}_{1,\theta}[\mathbf{A}_p]\mathscr{R}_{adm}\Bigg)\mathbf{v}_{max}[\mathbf{A}_p],$$

where we furthermore made use of the identity $\frac{\partial}{\partial x}\mathbf{X}^{-1} = -\mathbf{X}^{-1}(\frac{\partial}{\partial x}\mathbf{X})\mathbf{X}^{-1}$. The gradient at $\mathbf{A}_p = \overline{\mathbf{A}}_p$ is then easily found with (4) by evaluating the above equation for all $\{A_{p,m}\}_{m=1}^M$ at $\overline{\mathbf{A}}_p$. Note that the gradient of $\mathscr{P}_{1,\theta}[\mathbf{A}_p]\mathscr{R}_{adm}$ can be calculated analytically, whereas the gradient of $\mathscr{P}_{1,\theta}^{1/2}[\mathbf{A}_p]\mathscr{R}_{adm}\mathscr{P}_{1,\theta}^{1/2}[\mathbf{A}_p]$ cannot. This observation motivated the last step taken in Lemma 1, see also Remark 1.

Since (37) is not dependent on ϕ_p, we trivially have that the gradient $\nabla_{\phi_p}\lambda_{max}\left(\mathscr{P}_{1,\theta}[\mathbf{A}_p]\mathscr{R}_{adm}\right) = \mathbf{0}$.

Constraints (34): The derivatives of the constraints are now calculated. Following [10] the functions $f_{u,p}$ and $f_{y,p}$ in (34) are written as

$$f_{u,p}(\mathbf{A}_p, \phi_p) = \eta_{u,p}^T\eta_{u,p},\ f_{y,p}(\mathbf{A}_p, \phi_p) = \eta_{y,p}^T\eta_{y,p},$$

with $\eta_{u,p}[l] = u_r^k[l]/u_{r,max}^k$, $\eta_{y,p}[l] = y_r^k[l]/y_{r,max}^k$, $k = p/2$, and $\dim(\eta_{u,p}) = \dim(\eta_{y,p}) = L+1$. The derivatives of these functions with respect to the amplitudes and phases are then easily found:

$$\frac{\partial f_{u,p}}{\partial A_{p,m}} = 2\eta_{u,p}^T\frac{\partial \eta_{u,p}}{\partial A_m},\ \frac{\partial f_{u,p}}{\partial \phi_m} = 2\eta_{u,p}\frac{\partial \eta_{u,p}}{\partial \phi_{p,m}},$$
$$\frac{\partial f_{y,p}}{\partial A_{p,m}} = 2\eta_{y,p}^T\frac{\partial \eta_{y,p}}{\partial A_{p,m}},\ \frac{\partial f_{y,p}}{\partial \phi_m} = 2\eta_{y,p}\frac{\partial \eta_{y,p}}{\partial \phi_{p,m}},$$

in which

$$\frac{\partial \eta_{u,p}}{\partial A_{p,m}}[l] = k\frac{u_r^{k-1}[l]}{u_{r,max}^k}|S_0(z_m)|\sin(\omega_m l\Delta L + \phi_{p,m} + \phi_S),$$
$$\frac{\partial \eta_{u,p}}{\partial \phi_{p,m}}[l] = k\frac{u_r^{k-1}[l]}{u_{r,max}^k}A_{p,m}|S_0(z_m)|\cos(\omega_m l\Delta L + \phi_{p,m} + \phi_S),$$

in which $\phi_S = \angle S_0(z_m)$. The derivatives for $\eta_{y,p}$ can be found analogously.